
Article:

Yu, L. orcid.org/0000-0002-6109-7462, Luo, X. orcid.org/0000-0002-9546-0960, Croft, H. orcid.org/0000-0002-1653-1071 et al. (2 more authors) (2024) Seasonal variation in the relationship between leaf chlorophyll content and photosynthetic capacity. Plant, Cell & Environment, 47 (10). pp. 3953-3965. ISSN 0140-7791

https://doi.org/10.1111/pce.14997

Received: 28 January 2024 | Revised: 13 May 2024 | Accepted: 28 May 2024

DOI: 10.1111/pce.14997

ORIGINAL ARTICLE

Plant, Cell & Environment | WILEY

Seasonal variation in the relationship between leaf chlorophyll content and photosynthetic capacity

Liyao Yu[1] | Xiangzhong Luo[1] | Holly Croft[2] | Cheryl A. Rogers[3] | Jing M. Chen[4]

[1]Department of Geography, National University of Singapore, Singapore, Singapore

[2]School of Biosciences, University of Sheffield, Sheffield, UK

[3]Department of Geography and Environmental Studies, Toronto Metropolitan University, Toronto, Canada

[4]Department of Geography and Planning, University of Toronto, Toronto, Canada

Correspondence

Liyao Yu and Xiangzhong Luo, Department of Geography, National University of Singapore, 1 Arts Link, Singapore 117570, Singapore.
Email: liyaoyu@nus.edu.sg and xzluo.remi@nus.edu.sg

Funding information

National University of Singapore; UK Research and Innovation (UKRI) Future Leader

Abstract

Accurate estimation of photosynthesis is crucial for ecosystem carbon cycle modelling. Previous studies have established an empirical relationship between photosynthetic capacity (maximum carboxylation rate, V_{cmax}; maximum electron transport rate, J_{max}) and leaf chlorophyll (Chl) content to infer global photosynthetic capacity. However, the basis for the Chl-V_{cmax} relationship remains unclear, which is further evidenced by the temporal variations in the Chl-V_{cmax} relationship. Using multiple years of observations of four deciduous tree species, we found that V_{cmax} and J_{max} acclimate to photosynthetically active radiation faster (4–8 weeks) than Chl (10–12 weeks). This mismatch in temporal scales causes seasonality in the V_{cmax}-Chl relationship. To account for the mismatch, we used a Chl fluorescence parameter (quantum yield of Photosystem II, Φ(II)) to tighten the relationship and found Φ(II) × Chl correlated with V_{cmax} and J_{max} (r^2 = 0.74 and 0.72 respectively) better than only Chl (r^2 = 0.7 and 0.6 respectively). It indicates that Φ(II) accounts for the short-term adjustment of leaf photosynthetic capacity to light, which was not captured by Chl. Our study advances our understanding of the ecophysiological basis for the empirical V_{cmax}-Chl relationship and how to better infer V_{cmax} from Chl and fluorescence, which guides large-scale photosynthesis simulations using remote sensing.

KEYWORDS

chlorophyll fluorescence, J_{max}, light acclimation, optimality theory, V_{cmax}

1 | INTRODUCTION

Global photosynthesis is the largest carbon flux on the land surface (Friedlingstein et al., 2022), removing CO_2 from the atmosphere and contributing to carbon neutrality and climate change mitigation. Our current estimate of global photosynthesis relies heavily on process-based models, however, they often provide estimates varying in a wide range (110–170 Pg C year^{-1}) (Anav et al., 2015; Piao et al., 2013; Ryu et al., 2019), and a main source of the uncertainty is the lack of constraint on leaf photosynthetic capacity over large scales (Rogers et al., 2017; Walker et al., 2017). Photosynthesis at the leaf level has been overwhelmingly modelled using the Farquhar-von Caemmerer-Berry (FvCB) biochemical model (Farquhar et al., 1980; von Caemmerer, 2000). It characterises photosynthetic limitations in the

Calvin-Benson Cycle with two parameters: the maximum carboxylation rate (V_{cmax}) and the maximum electron transport rate (J_{max}). V_{cmax} is related to the content and activity of the photosynthetic enzyme Ribulose-1,5-bisphosphate (RuBP) carboxylase/oxygenase (Rubisco), while J_{max} reflects the capacity of RuBP regeneration reduced by Nicotinamide adenine dinucleotide phosphate. Both V_{cmax} and J_{max} have been found to vary temporarily and spatially under the influences of climatic and nutritional variables and leaf developmental stages (Kattge & Knorr, 2007; Walker et al., 2017). Therefore, acquiring accurate V_{cmax} and J_{max} (scaled to 25°C) is critical for improving the simulation of global photosynthesis (Rogers, 2014).

However, V_{cmax} is usually determined from in-situ measurement of the photosynthesis-CO_2 (A/C_i) response curves, which is time-consuming and has limited spatial representation. Efforts to extrapolate V_{cmax} using remote sensing data have drawn much attention (Chen et al., 2022) and led to several approaches, that is, using leaf nitrogen content (Kattge et al., 2009), leaf chlorophyll (Chl) content (Croft et al., 2017; Luo et al., 2019; Wang et al., 2020), or sun-induced fluorescence (SIF) (Liu et al., 2023) as a proxy. Chl, the pigment that harvests photons and excites electrons to drive the regeneration of RuBP, is a critical component of leaf photochemistry and thus can reflect the photosynthetic capacity to some extent. One advantage of using Chl as a proxy for V_{cmax} estimation is that the pigment has unique spectral characteristics that can be utilised for large-scale estimation using remote sensing. Multiple global Chl maps have been developed (Croft et al., 2020; Xu et al., 2022) to facilitate the application of Chl in carbon cycle modelling.

However, several knowledge gaps remain regarding the empirical relationship between V_{cmax} and Chl:

(1) The relationship between Chl and V_{cmax} varies seasonally. Previous studies have reported that Chl can track the seasonal variation in V_{cmax} (Chen et al., 2022; Croft et al., 2017), and some even suggested a universal Chl-V_{cmax} relationship (Lu et al., 2022; Qian et al., 2021; Wang et al., 2020). While we acknowledge that Chl has demonstrated to be a good proxy for V_{cmax} (mostly $r^2 > 0.5$), we nevertheless notice that there are instances where variations in V_{cmax} were not fully accounted for by Chl (Li et al., 2020; Li et al., 2022; Warren, 2006), suggested by the varying r^2 values (0.29–0.76) from these studies. This mismatch of Chl and V_{cmax} implies a nonproportional use of resources (i.e., nitrogen) for light harvesting and Calvin-Benson Cycle reactions. The seasonal variation in the V_{cmax}-Chl relationship is further corroborated by the fact that V_{cmax} shows a higher level of plasticity than Chl in response to environmental factors, in particular, light conditions (Poorter et al., 2019; Yu et al., 2022), suggesting more limited Chl acclimation than V_{cmax}. We, therefore, hypothesise that the seasonal variation in the Chl-V_{cmax} relationship is due to the different speeds (i.e., time scales) at which Chl and V_{cmax} acclimate to changes in photosynthetic active radiation (PAR).

(2) The basis of the empirical Chl-V_{cmax} relationship remains unclear. V_{cmax} is determined by the amount and activity of Rubisco, the most important protein in leaves. Rubisco occupies up to 40% of the total leaf nitrogen (Taiz et al., 2018). Meanwhile, the production of Chl also needs nitrogen. That understanding motivates some studies to adopt linear relationships between Chl and V_{cmax} based on their covariations with leaf total nitrogen content (Croft et al., 2017; Houborg et al., 2015; Luo et al., 2018; Qian et al., 2021). However, leaf total nitrogen is not only used for Rubisco and Chl but used for non-photosynthetic components (i.e., supporting structures such as cell walls). The allocation of leaf total nitrogen to nonphotosynthetic components contributes to a loose relationship between leaf total nitrogen content and photosynthetic parameters (i.e., V_{cmax} and Chl), especially during the transition period where leaf and canopy structure changes (Warren, 2006). Loose correlations between leaf total nitrogen and Chl have been reported in common bean, giant taro, sunflower, and maize (Miner & Bauerle, 2019; Seemann et al., 1987). These studies suggest that the dynamic allocation of nitrogen and kinetics of Rubisco may contribute to the uncertainty in relating Chl to V_{cmax} through leaf total nitrogen content.

Another line of thought suggests that Chl is directly related to J_{max} (Alton, 2017), as the photons absorbed by the pigment are used to activate electron transport for photosynthesis (Evans & Poorter, 2001). The Chl-J_{max} relationship can be further used to infer a Chl-V_{cmax} relationship due to the tight coordination of J_{max} and V_{cmax} following optimised resource distribution between carboxylation and electron transport (Chen et al., 1993; Wullschleger, 1993). Although this line of thought seems to have a stronger theoretical base than the nitrogen-based explanation, the Chl-J_{max} relationship is not always as strong as expected in some studies (Alton, 2017). Considering that the total electron transport rate consists of linear electron flow and cyclic electron flow, and only the former is used for RuBP regeneration in the Calvin-Benson Cycle, we suspect that there is a need to account for the portion of photons that are only used to activate the linear electron flow/photosynthesis to fully establish the Chl-J_{max} relationship. Since photosystems (PS) are the sites where photons are used to excite electrons, we propose that the quantum yield of PSII (Φ(II), determined by Chl fluorescence) is a potential proxy of the portion of the photons used for linear electron flow, and can be used to improve the Chl-J_{max} relationship. Here we did not consider the quantum yield of PSI as it remains largely constant (Sonoike, 2011).

In this study, we aim to address the above two knowledge gaps and test the proposed hypotheses. To do so, we used multiple years (2013–2018) of the in-situ observations of Chl, leaf photosynthetic capacity, and Chl fluorescence of four deciduous tree species in a mixed forest in Canada, in combination with a photosynthetic optimality theory to examine the Chl, $V_{cmax,}$ and J_{max} relationships. By addressing the gaps, we provide a robust theoretical basis to explain the empirical relationship between Chl and V_{cmax} and offer guidance for its improvement and application over large scales.

2 | MATERIALS AND METHODS

2.1 | Site measurement information

The Borden Forest Research Station is located in a mixed temperate forest in southern Ontario (44°19'N, 79°56'W), Canada. It lies in a

transition zone between northern boreal species and southern temperate species, therefore, it has been identified as susceptible to climate change and represents a region of ecological significance. The mean annual air temperature (T) is approximately 7.4°C and the mean annual precipitation is approximately 784 mm (Froelich et al., 2015). The mean canopy height is 22 m, with dominant deciduous tree species including bigtooth and trembling aspen (*Populus grandidentata* Michx. and *Populus tremuloides* Michx.), red maple (*Acer rubrum* L.), and white ash (*Fraxinus americana* L.)

We used the local half-hourly meteorological data, that is, PAR, T, and relative humidity (RH), recorded at a 33 m height from a 44 m flux tower during the 2013-2018 growing seasons. We calculated VPD using T and RH. We showed the daily-averaged daytime PAR, T, and VPD in Supporting Information S1: Figure 1.

For each data collection in the growing seasons during 2013–2018, five leaves from a tree of each of the four investigated species were sampled approximately every 10 days. We collected these leaves at the top of the canopy from the neighbouring flux tower to exclude the influence of light gradients within the canopy on leaf biochemical and photosynthetic properties. We collected leaf samples using a puncher which can punch standard 1 cm^2 samples from the leaf, extracted pigments (Chl *a*, *b*, and carotenoids [Car]) from leaf samples using *N*,*N*-dimethylformamide, measured the absorptance at 663.8, 646.8, and 480.0 nm using a Shimadzu UV-1700 photospectrometer, and calculated Chl *a*, *b*, and Car per unit leaf area (μg cm^{-2}) following Croft et al. (2017). In 2014–2018, we conducted photosynthesis-CO_2 (A-C_i) curves and determined leaf photosynthetic parameters (V_{cmax} and J_{max}, μmol m^{-2} s^{-1}) using an LI-6400XT portable infra-red gas analyser (Li-Cor) with a R/B light source (6400-02B). A-C_i curves were recorded under a leaf temperature of 25°C, a saturating red/blue (R/B, 9:1) light with a photosynthetic photon flux density (PPFD) of 1800 μmol m^{-2} s^{-1}, an RH between 40% and 80%, a flow rate of 300 μmol m^{-2} s^{-1}, and 10 step-wised ambient CO_2 concentrations from 50 to 1800 μmol m^{-2} s^{-1}. To maintain repeatable measurements in the growing seasons, we used leaves from the same branches as were used in pigment measurements on the same day. In 2016 and 2018, we also recorded Chl fluorescence using an LI-6400XT with a fluorometer (6400-40 LCF, Li-Cor). Φ(II) was determined following Schreiber et al. (1986) and Genty et al. (1989). We set the measuring light with an intensity of 3 μmol m^{-2} s^{-1} and a rate of 0.25 kHz, the saturating pulse with an intensity of 6000 μmol m^{-2} $s^{-1,}$ and a duration of 0.8 s. To stimulate comparable levels of fluorescence throughout a growing season, we set consistent actinic light at 1800 μmol m^{-2} s^{-1}, which is similar to the daily peak sunlight PPFD experienced by top-canopy leaves and beyond saturating PPFD for photosynthesis. We did not sample trembling aspen in 2018 because no branch of this species could be safely reached from the neighbouring flux tower. The data we used were a combination of the data set previously published in Croft et al., 2017 (i.e., weekly V_{cmax}, J_{max}, and Chl in 2013–2015) and the data set we acquired at the same site after 2015 for this study (i.e., weekly V_{cmax}, J_{max}, and Chl in 2016–2018, and the Chl fluorescence data in 2016 and 2018). The Croft data set (2013–2015) has been widely used in various studies on the seasonal dynamic of leaf Chl content and photosynthetic capacity (e.g., Jiang et al., 2020; Qian et al., 2021).

2.2 | Determination of temporal scales at which Chl and V_{cmax} acclimate to light

To determine the temporal scales at which Chl acclimates to light, first, we calculated the average PAR and other climate variables over different time windows, namely from 1 week to 12 weeks (with a 1-week step) before the date of each measurement. To obtain the temporal scale of light acclimation for Chl, we calculated the correlation coefficient (r) of Chl and average PAR from the varying time windows. The time window that shows the largest r^2 indicates the likely time scale of light acclimation for Chl. We did not incorporate T and VPD into the correlation because there have been debates on whether these factors would impact Chl (Bachofen et al., 2020; Dusenge et al., 2020; Goto et al., 2021; Kong et al., 2021; León-Chan et al., 2017). Indeed, the r^2 values from the multiple regressions of Chl to PAR, T, and VPD show limited variation, indicating that the multiple regression approach is unsuitable for determining the temporal scale of Chl acclimation (Supporting Information S1: Figure 2). When we attempted to obtain the temporal scale of light acclimation for V_{cmax}, we did not examine the r^2 between V_{cmax} with the average PAR as other climate factors (i.e., T and VPD) impose confounding impacts on V_{cmax}. Instead, we used a photosynthesis optimality model (see below) to first acquire many versions of simulated V_{cmax} (V_{cmax_s}) using average PAR and other climate variables across different time durations (i.e., 1–12 weeks before the measurement), and then obtain the r^2 between V_{cmax_s} and measured V_{cmax} for each time duration. The time duration that shows the largest r^2 indicates the temporal scale of light acclimation for V_{cmax}. The optimality model has been proven to be robust to simulate V_{cmax} on our study site—the Borden forest (Jiang et al., 2020) and to capture the light acclimation effect to the maximum photosynthetic capacity (A_{max}) across different ecosystems (Luo & Keenan, 2020). We also provided the values of r^2 from the multiple correlations of V_{cmax} to PAR, T, and VPD in Supporting Information S1: Figure 2.

2.3 | The photosynthesis optimality model

The optimality model was developed by Smith et al. (2019), based on the coordination theory (Chen et al., 1993) and the least-cost hypothesis (Prentice et al., 2014). The coordination theory states that carboxylation and electron transport equally constrain photosynthesis under average environmental conditions. The least-cost hypothesis posits that plants optimise their resource investment to maintain a given photosynthetic rate at the least transpirational cost. Smith et al. (2019) used PAR, T, VPD, and elevation (as the index of atmospheric pressure) to drive the optimality model. They found that this model captures 64% of the variability in field-measured V_{cmax} across the global scale, suggesting that climate (especially light

availability) is the first driver of global photosynthetic capacity. This model has been validated not only with global remote-sensing derived V_{cmax} ($r^2 = 0.55$, Chen et al., 2022) but also by Jiang et al. (2020) at the same site as this study, in which they show a tight correlation between modelled and observed V_{cmax} ($r^2 = 0.66$). We input average daytime PAR, T, and VPD in varying time windows (1–12 weeks before the measurement) into the optimality model to estimate the optimal V_{cmax} and J_{max} then took each of the 12 sets of optimal V_{cmax} and J_{max} to correlate with the measured V_{cmax}.

2.4 | Improving the Chl-V_{cmax} relationship by incorporating Chl fluorescence

Evans and Poorter (2001) found that the number of photons harvested by a leaf, reflected by the absorptance, correlates positively to Chl. However, not all harvested photons are used for photosynthesis. Based on our hypothesis, we incorporated the Φ(II) in the Chl-J_{max} relationship, to consider only the proportion of energy from the harvested photons used to drive photochemistry through the linear electron flow, while the rest is dissipated through the cyclic electron flow or as heat. Therefore, the Chl-J_{max} relationship could be theoretically expanded to $J_{max} = a \times R(PSII) \times \Phi(II) \times Chl + b$, in which a is the coefficient of independent variables, R(PSII) is the portion of harvested photons distributed to PSII, and b is a constant. Here, we assume R(PSII) equals 0.5. This equation is inspired by a mechanistic equation of $ETR = R(PSII) \times \Phi(II) \times PPFD_a$ (Genty et al., 1989), in which ETR is the electron transport rate, $PPFD_a$ is the absorbed photosynthetic photon flux density. This equation has been widely used to determine ETR by Chl fluorescence (Maxwell & Johnson, 2000). We adopted this equation here empirically by assuming that (1) ETR and Jmax reflect electron transport capacity at different aspects and (2) $PPFD_a$ and Chl should be proportional as well. We also expanded the Chl-V_{cmax} relationship to $V_{cmax} = c \times R(PSII) \times \Phi(II) \times Chl + d$.

2.5 | The estimation of Chl redundancy and stomatal slope parameter

According to previous studies (Poorter et al., 2019; Yu et al., 2022), Chl is less sensitive to PAR levels in comparison to V_{cmax} (and J_{max}). Since plants have evolved to optimise their carbon gain under continuously fluctuating light conditions in nature, this suggests that there might be redundant Chl existing in leaves, the extent of which could be reflected by the dynamic regulation of Φ(II). Previous studies found that mutants with deficient Chl tend to show higher Φ(II), in some cases accompanied by unaffected photosynthesis (Gu et al., 2017; Li et al., 2013), implying a negative relationship between Φ(II) and redundancy in Chl. Moreover, Φ(II) exhibits seasonal variations with higher levels in the middle of the growing seasons (suggested by the overall positive correlation between PAR and Φ(II), Supporting Information S1: Figure 7), suggesting a lower Chl redundancy than the beginning and end of growing seasons when light and thermal conditions are suboptimal. In this study, we intend to preliminarily quantify the Chl redundancy as follows:

First, we assume that Chl is the least redundant when Φ(II) reaches its maximum in a growing season. We calculated the "theoretically optimal" Chl using $Chl_o = Chl_m \times \Phi(II)_{max}/\Phi(II)_m$, in which Chl_o and Chl_m are the estimated optimal and measured Chl for each of the four species respectively; $\Phi(II)_{max}$ and $\Phi(II)_m$ are the maximum Φ(II) in the growing season and measured Φ(II) on the same day when Chl and V_{cmax} were measured.

Then, we calculated the degree of redundancy (Chl_Rd) as $Chl\_Rd = (Chl_o - Chl_m)/Chl_o$. Note that here we focus on the relative Chl_Rd across the four species, as the Chl_Rd calculated here might not reflect the absolute magnitude of Chl_Rd for two reasons. First, the level of Φ(II) is dependent on the PAR of the actinic light used in the fluorescence measurement, therefore the Φ(II) values are incomparable across studies if different PAR is used. Second, we did not obtain continuous $\Phi(II)_{max}$ observations for the whole growing season as Φ(II) was only sampled around the noons in fieldwork days (approximately every 10 days). Nevertheless, the data that we have are adequate to infer the relative difference in Chl_Rd among species, considering their Φ(II) were measured at the same time and under the same PAR.

Stomatal conductance (g_s) plays a critical role in the global carbon cycle by linking transpiration (E) and photosynthesis (A) and has been found to be optimised to the given environment (C_a, PAR, VPD, and T) (Cowan & Farquhar, 1977; Wong et al., 1979). Modelling the dependence of g_s on environmental factors requires the stomatal slope parameter (g_1) (Medlyn et al., 2011). g_1 is inversely proportional to the carbon cost per water use or the water use efficiency (WUE, evaluated as A/E, Davidson et al. (2023)) and varies largely among PFTs and under different climates (Lin et al., 2015), potentially reflecting the strategy of plants to balance carbon gain and water loss. A low value of g_1 indicates that the plant is likely to be conservative in its water use or has a higher WUE. Therefore we suspect that there would be a relationship between Chl_Rd and g_1, considering that g_1 and Chl redundancy are both relevant to the optimal cost and gain of carbon. To test this, we first calculated g_1 as $g_1 = g_s \times C_a \times \sqrt{VPD}/(1.6 \times A) - \sqrt{VPD}$ then correlated the medians of Chl_Rd and g_1 for the four species.

2.6 | Statistical analyses

All statistical analyses were conducted in R (R Core Team, ver. 4.3.1). We checked the normality of the data with Shapiro-Wilk's method and found that Chl_Rd of trembling aspen and white ash and g_1 of red maple in 2016 did not follow normality. Therefore, we performed the Kruskal–Wallis (K-W) test on Chl_Rd and g_1

and multi-comparison among species with the pairwise Wilcox test.

3 | RESULTS

3.1 | Seasonality in the Chl-V_{cmax} relationship

Across the four species measured during 2013–2018, the ratio of V_{cmax} to Chl (i.e., V_{cmax}/Chl ratio) exhibits large variation over the growing season (Figure 1), ranging from 0.58 to 2.71. Although there was no significant trend in the V_{cmax}/Chl ratio of any species ($p > 0.05$), all species except bigtooth aspen showed the highest mean V_{cmax}/Chl ratio at the start of the growing season (2.04 for red maple, 1.75 for trembling aspen, and 2.50 for white ash) and the lowest mean V_{cmax}/Chl ratio at the end of the growing season (1.36 for trembling aspen, 1.32 for trembling aspen, and 1.47 for white ash) except red maple.

3.2 | Chl acclimates to light slower than V_{cmax}

We determined the temporal scale of Chl acclimation by comparing r^2 values from regression of Chl to average PAR of different time durations (i.e., 1–12 weeks before the measurement) (Supporting Information S1: Figure 3). The lower r^2 values under the 1–4 week durations indicated that Chl was not sensitive to changes in short-term PAR. The maximum r^2 occurs under greater time durations, specifically 12 weeks for bigtooth aspen and red maple, 11 weeks for trembling aspen, and 10 weeks for white ash (Figure 2). In contrast, the correlations between modelled and measured V_{cmax} (or J_{max}) have the highest r^2s when using average PAR in the recent 4–8 weeks (Figure 2 and Supporting Information S1: Figure 4), indicating that V_{cmax} acclimates to PAR at the temporal scale of roughly 1 month, except J_{max} of trembling aspen. Moreover, the temporal scale at which V_{cmax} acclimates to light was shorter than that of J_{max} (Figure 2a,b,c), except for white ash (Figure 2d), supported by the higher r^2 values from V_{cmax} estimation than J_{max} at scales <4–6 weeks.

3.3 | Incorporating Φ(II) improved J_{max} and V_{cmax} estimation

Based on our hypothesis that incorporating Φ(II) could strengthen the Chl-J_{max} (and V_{cmax}) relationship, we tested whether Chl × Φ(II) indicates the dynamics in J_{max} better than Chl alone using 2 years of data. We found that the correlation of J_{max} to Chl × Φ(II) had r^2 values of 0.72 and 0.61 for 2016 and 2018 respectively (Figure 3b, $p < 0.001$), which were greater than those of 0.6 and 0.51 (Figure 3a, $p < 0.001$) from correlating J_{max} to Chl alone. The r^2 values for the correlation between V_{cmax} and Chl × Φ(II) (0.74 and 0.55, Figure 3d,

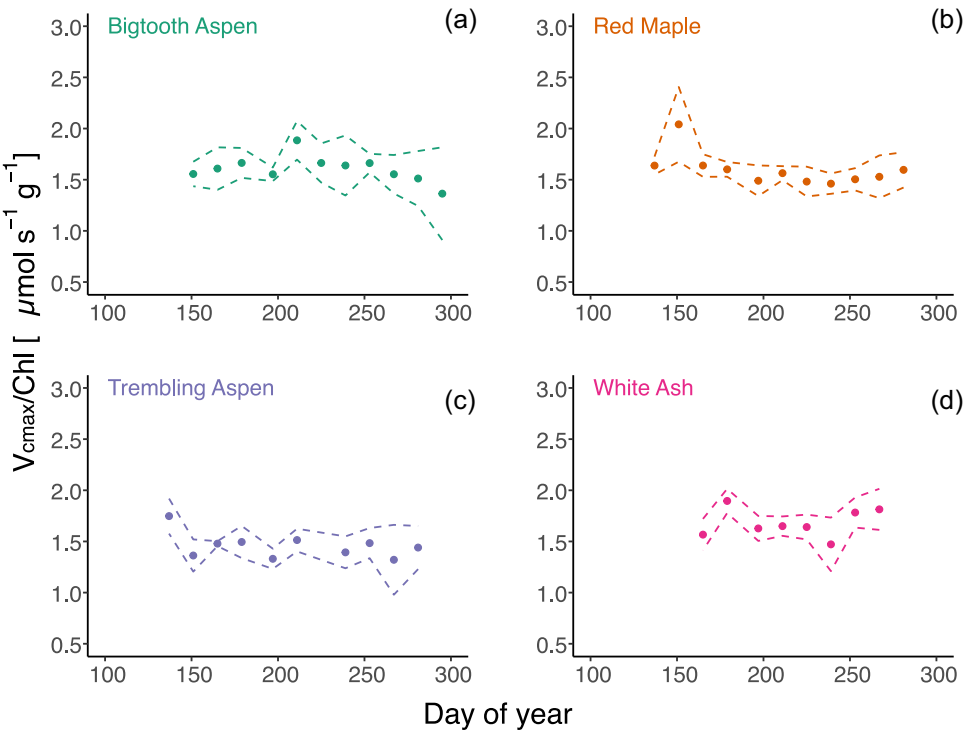

FIGURE 1 Seasonal variation in the ratio of V_{cmax} (μmol m^{-2} s^{-1}) to leaf Chl content (μg cm^{-2}) for four species in 2014–2018: (a) Bigtooth aspen, (b) Red maple, (c) Trembling aspen, and (d) White ash. Days of year are grouped with a 2-week step. Dashed lines indicate interannual variations in V_{cmax}/Chl (mean ± standard error). Data in groups with $n < 2$ are not shown. Solid lines indicate the regressions of V_{cmax}/Chl on the day of year (grouped in a 2-week duration). [Color figure can be viewed at wileyonlinelibrary.com]

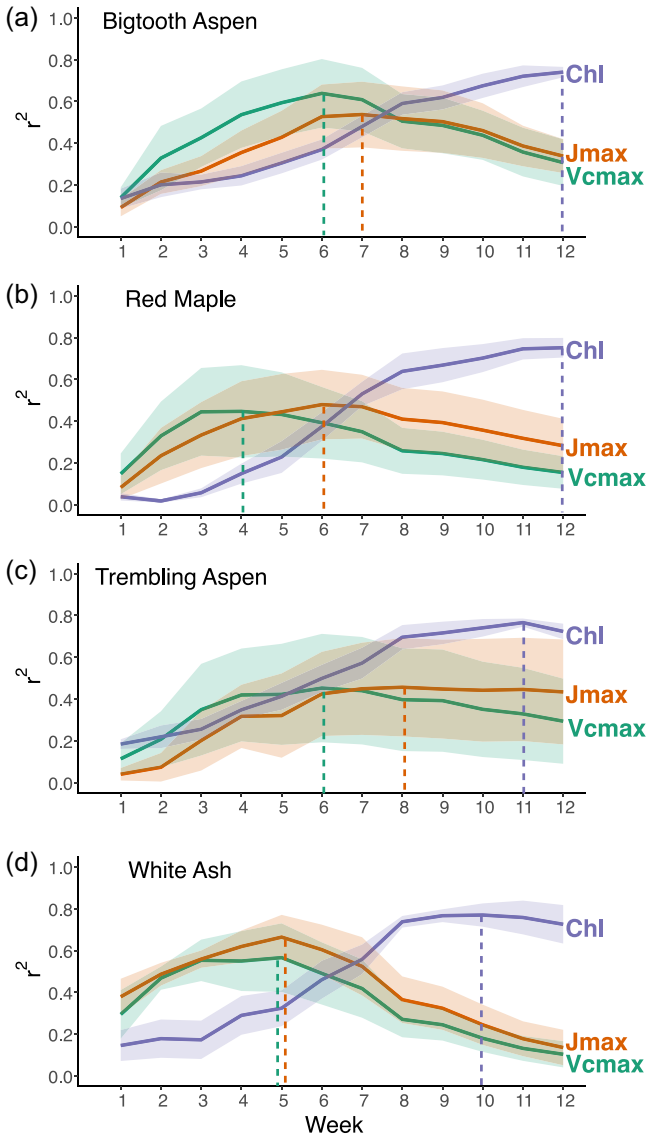

FIGURE 2 Summary of determination coefficients (r^2) from the linear correlation between (1) Chl and PAR (2) modelled and measured V_{cmax} and (3) modelled and measured J_{max} in the recent 1–12 weeks for four species in 2013–2018: (a) Bigtooth aspen, (b) Red maple, (c) Trembling aspen, and (d) White ash. Lines show the mean value from four species in 4–5 years and the shaded areas indicate the uncertainty over years (mean ± standard error). The dotted lines indicate the shortest temporal scale at which the r^2 is the highest. Chl, chlorophyll; PAR, photosynthetic active radiation. [Color figure can be viewed at wileyonlinelibrary.com]

$p < 0.001$) were also greater than those between V_{cmax} and Chl (0.7 and 0.52, Figure 3c, $p < 0.001$).

3.4 | Redundancy in Chl

We further examined the redundancy in Chl (Chl_Rd) in 2016 and 2018. We found that red maple showed the highest Chl_Rd (median: 24.44% and 37.02% for 2016 and 2018 respectively; the amount of redundant Chl in the percentage of required Chl for leaves) and white ash showed lower values (median: 10.68% and 31.75%) (Figure 4a). The Chl_Rd of bigtooth aspen was at 14.53% and 26.11% for 2016 and 2018 respectively. The Chl_Rd of trembling aspen was at 15.87% for 2016. We did not find a significant inter-specific variation ($p = 0.94$ and 0.27). We also extracted g_1, the stomatal slope parameter, which is inversely related to WUE. In 2016, bigtooth aspen had the highest median of g_1 (1.78), followed by white ash (1.64), while red maple and trembling aspen had largely lower g_1 (0.98 and 1.16 respectively, Figure 4b). The inter-specific variation in g_1 was statistically significant ($p = 0.005$). In 2018, bigtooth aspen also had the largest median of g_1 (3.61), followed by white ash (median: 2.75), while red maple had the lowest median of 2.42, although the differences were not significant ($p = 0.14$, Figure 4b). Then we correlated the medians of Chl_Rd and g_1 in the growing season of 2016 and 2018, and found that Chl_Rd demonstrated weak and negative correlations with g_1, with r^2 values of 0.64 and 0.91, respectively, (both $p = 0.19$, Figure 4c).

4 | DISCUSSION

In this study, we demonstrate that the mismatch in temporal scales at which V_{cmax} (and J_{max}) and Chl acclimate to light contributes to the seasonality in the Chl-V_{cmax} (and J_{max}) relationship. We also developed a novel approach to improve the Chl-V_{cmax} (and J_{max}) relationship by taking into account the portion of harvested light energy by leaves that is used for photosynthetic carbon assimilation.

4.1 | Temporal scale of light acclimation

In this study, we found that the temporal scale of light acclimation for Chl (9–12 weeks) is longer than that for V_{cmax} (4–6 weeks). Although the acclimation of leaf traits to environmental conditions has been well recorded by many studies (Björkman & Holmgren, 1963; Boardman, 1977; Oguchi et al., 2005; Pearcy et al., 1996; Poorter et al., 2019; Terashima et al., 2001), the exact temporal scale of the acclimation remains poorly studied. Yu et al. (2022) found photosynthesis (V_{cmax} and J_{max}) of cucumber seedlings acclimates to a change in PAR with a longer time lag than morphology (leaf mass per area), implying a difference in the temporal scales of acclimation for leaf structural traits and physiological traits. Our study further advances this finding, reporting that even within the leaf physiological traits (i.e., V_{cmax}, J_{max}, and Chl), there is a difference in the temporal scale of light acclimation.

Lu et al. (2022) found that the response of leaf Rubisco content to changes in PAR is three times larger than that of Chl, leading to a sensitivity of Rubisco/Chl to light. Our study provides a new perspective: inconsistency in both the magnitude of acclimation of Chl and Rubisco, and a mismatch in the temporal scale of this acclimation contributing to seasonal variation in the relationships between Chl/V_{cmax} and Chl/Rubisco.

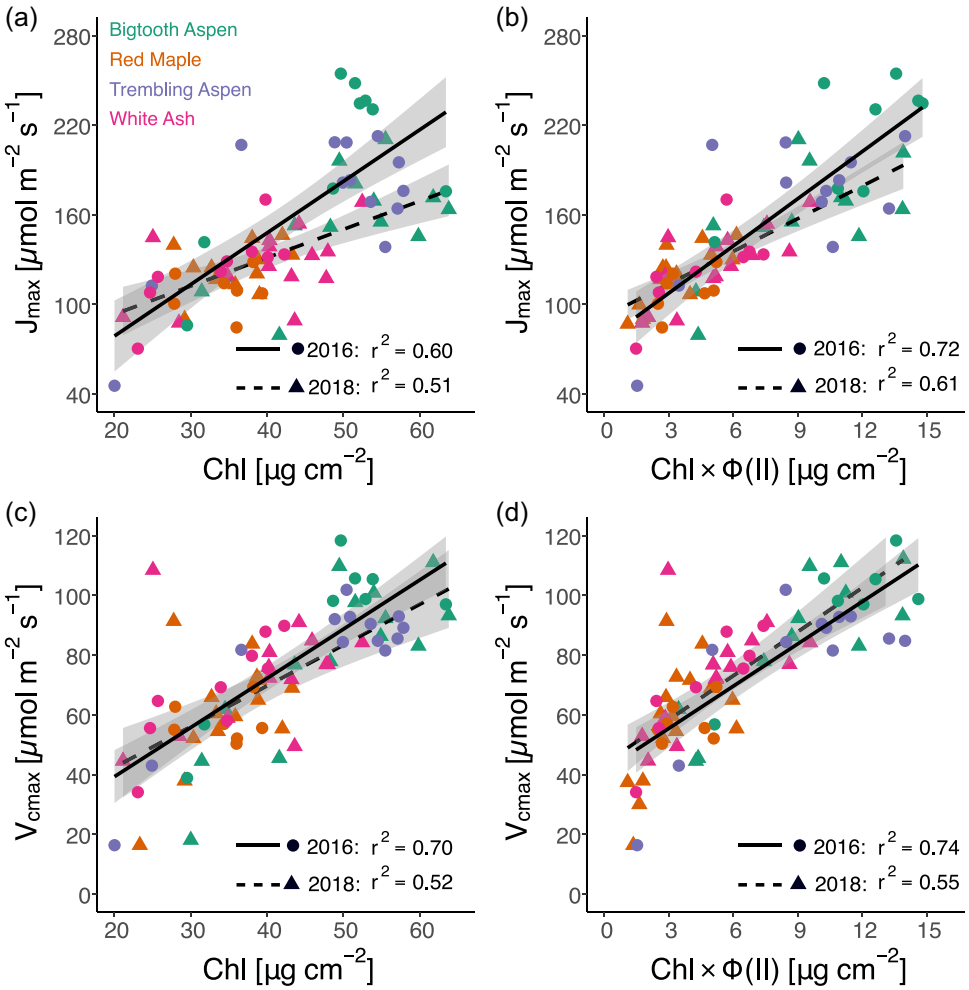

FIGURE 3 Regression of J_{max} on (a) leaf Chl content (μg cm^{-2}) or (b) product of leaf Chl content multiplied by the quantum yield of photosystem II (Φ(II)), Chl × Φ(II) and of V_{cmax} on (c) Chl or (d) Chl × Φ(II). Data in two years (2016: circles; 2018: triangles) were used. Regression lines (2016: solid; 2018: dashed) and confidence intervals (shaded areas) are shown. [Color figure can be viewed at wileyonlinelibrary.com]

4.2 | Contribution of leaf acclimation and ontogeny to the variation in V_{cmax} and Chl

Seasonal variations in leaf photosynthetic traits of the species from temperate forest sites may result from acclimation to the environmental gradients and/or ontogenetic development of leaves (Yamashita et al., 2002). So far, conclusions on to what extent these two mechanisms contribute to the changes in leaf traits remain ambiguous (McConnaughay & Coleman, 1999; Xie et al., 2012). If the changes are solely due to the ontogenetic process of the leaves, variations in leaf traits should be predictively presented as a function of leaf developmental or phenological phases, irrespective of the environment experienced by the leaves (Evans, 1972). Our preliminary analysis, however, does not support this explanation as the ratio of V_{cmax} to Chl in 2016 is significantly higher than the ratios in the other 3 years, while the average PAR in 2016 is significantly greater than the other 3 years (Supporting Information S1: Figure 5). This further implies that the variation in light environment, and therefore light acclimation, is responsible for the variation in the V_{cmax}/Chl ratio. The existence of light acclimation of V_{cmax} and Chl has also been demonstrated by Rodriguez-Calcerrada et al. (2008), who studied the influence of transferring oak seedlings from shaded to sun environments and vice versa, and found that both V_{cmax} and Chl are related to the current-year light environment. Moreover, they found that the impact of light acclimation exists regardless of the phenological phases (i.e., leaf flushing and full expansion of leaves). Uemura et al. (2000) confirmed the variation of photosynthetic capacity to light conditions. Shading leaves of two beech species for four continuous years, they found A_{max} (parallel to V_{cmax}) is related to current-year PAR (sun or shade). Therefore, although it remains difficult to distinguish the contributions of leaf acclimation and ontogeny to the seasonality of V_{cmax} and Chl, it is highly likely that leaf acclimation to the seasonal variations in light plays a significant role. Niklas (2006) presented an alternative point of view in which acclimation and ontogeny are not mutually independent because the rate of growth and development of leaves are subject to their

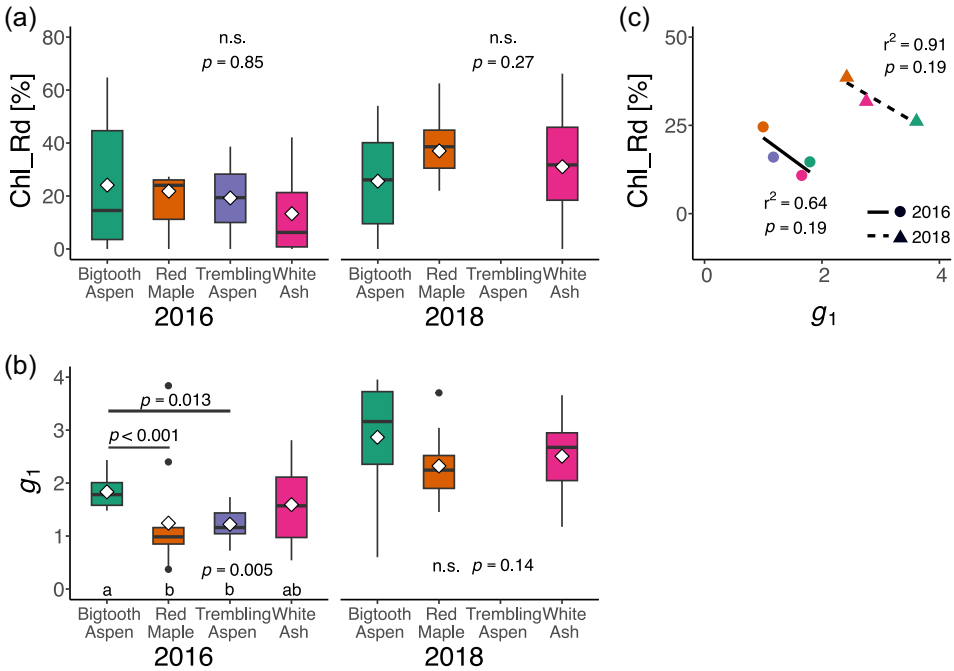

FIGURE 4 Redundancy in leaf Chl content (Chl_Rd, a), the stomatal slope parameter (g_1, b), and the correlation between monthly-aggregated medians of Chl_Rd and g_1 (c). Medians (bold lines), means (open diamonds), p values of the K-W test (a and b, $\alpha = 0.05$) and F-test (c, $\alpha = 0.05$), and regression lines (c) are shown. Data from two years (2016: circles and solid lines; 2018: triangles and dashed lines) were shown. Different letters in Figure (b) indicate the species which have significantly different g_1 ($p < 0.05$) by the pairwise Wilcox test ($\alpha = 0.05$). [Color figure can be viewed at wileyonlinelibrary.com]

adjustment to environmental factors, which perhaps explains why it is possible to predict the leaf photosynthetic capacity simply from climate (Smith et al., 2019). Therefore, while we acknowledge the role of leaf ontogenetic development in the seasonal variations in V_{cmax} and Chl, we suspect that it is unable to explain the mismatch of V_{cmax} and Chl without the consideration of light acclimation (Supporting Information S1: Figure 5), and at the seasonal scale, it is challenging to separate the role of ontogenetic development from climate impacts.

Meanwhile, we acknowledge that the relative importance of light acclimation might be subject to phenological stages. Light acclimation drives the plastic changes of leaf biochemical and physiological properties after leaves are out through the dynamic allocation of resources to Chl and V_{cmax}. However, other phenological stages, such as budburst and leaf senescence, are more likely relevant to the ontogeny process, as leaves are unable to sense the environmental conditions before their existence.

4.3 | Combining Chl and Chl fluorescence to infer V_{cmax}

In this study, we employed Φ(II) to improve the Chl-J_{max} relationship and then the Chl-V_{cmax} relationship, under the premise that Φ(II) is a good indicator of the percentage of photons absorbed by Chl and used for photosynthesis.

Φ(II) is sensitive to abiotic stresses, especially light intensity, temperature, and water availability (Sun et al., 2020; Walters & Horton, 1995; Yu et al., 2022). Studies have demonstrated that Φ(II) of *Acer pseudoplatanus* (Wyka et al., 2022), *Arabidopsis thaliana* (Chen et al., 2019), and *Cucumis sativus* (Yu et al., 2022) could acclimate to a reciprocal light regime (e.g., low to high PPFD) in less than 2 days, which is much shorter than Chl (De la Torre & Burkey, 1990). Therefore, the mismatch in the temporal scales of Vcmax (short) and Chl (long) acclimation could be mitigated by Φ(II) (very short) when calculating Chl×Φ(II), tightening V_{cmax}-Chl relationship. Since Φ(II) can be estimated from the Chl fluorescence, this new approach provides a novel opportunity to include fluorescence observations in V_{cmax} estimation. Although several studies have intended to use SIF for inferring V_{cmax} (Chen et al., 2022; He et al., 2019; Liu et al., 2023; Zhang et al., 2014), those are developed based on the empirical relationship between SIF and gross primary production and an inverted terrestrial biosphere model, without considering the physiological information of Φ(II).

The need for extracting Φ(II) of leaves with high accuracy and at a large spatial scale set a higher requirement for robust techniques of remote sensing. Traditionally, Φ(II) could only be determined by in situ measurement of single leaves with pulse-amplitude-modulation fluorometry, which is time-consuming and scale-limited and requires strict measurement light conditions. Recently, Wieneke et al. (2022) found Φ(II) could be determined by

combining the ratio ($F_{\uparrow ratio}$) of the two emitted SIF peaks (685 and 740 nm) and the photochemical reflectance index derived from remote sensing, indicating the potential of acquiring Φ(II) at ecosystem and global scales.

Other than using Φ(II), we also tested the possibility of using a statistical approach to improve the correlation between V_{cmax} (or J_{max}) and Chl. The statistical approach is based on the different temporal scales of light acclimation for V_{cmax} and J_{max} (mean: 6 weeks) and Chl (mean: 10 weeks), and we used the information to generate an empirical correction factor for Chl (Supporting Information S1: Figure 6). We found the statistical approach did not improve the correlations ($r^2 = 0.49$ and 0.64 respectively, Supporting Information S1: Figure 6b,c) compared to using Chl alone. We suspect that the reason why this empirical approach did not achieve an improvement is that we did not consider the inter-species difference in the acclimation rates.

4.4 | Does the plant maintain redundant Chl?

Our results in Figure 3 indicate that Chl is not strictly related to electron transport capacity. Instead, their relationship is mediated by Φ(II). Φ(II) seems to be positively correlated to the daily PAR (Supporting Information S1: Figure S7), indicating a greater extent of Chl redundancy at the beginning and end of the growing season, where light is not the limiting factor of photosynthesis. Wang et al. (2022) and Zhou et al. (2023) reported that rice mutants with less Chl reduce energy loss via nonphotosynthetic quenching and show higher Φ(II) and photosynthetic nitrogen use efficiency under an artificial light environment, implying that the actual Chl is more than the theoretical optimal. Why would plants invest nitrogen into Chl with a suboptimal strategy? One reasonable explanation might be that plants are faced with ubiquitous and incessant fluctuations in PAR and other environmental factors. Leaves with higher Chl could adjust their photochemistry and dissipate excess light energy through rapid xanthophyll cycles under fluctuating environmental conditions, such as between sun/shade phases, without the need to redistribute nitrogen between Chl and other components. This suboptimal strategy is also indicated by (Li et al., 2013), who found that mutants with less Chl did not have a higher portion of nitrogen allocated to Rubisco as expected, addressing the intrinsic uncertainty of using nitrogen as photosynthesis proxy.

Furthermore, our preliminary examination suggested a weak negative correlation between Chl_Rd and g_1 ($r^2 = 0.64$, $p = 0.19$, Figure 4c) among the four species, which implies a coordination between nutrient and water use across species. Species with a lower Chl_Rd suggest they use nutrients (e.g., nitrogen) more efficiently—as they do not have the resources to produce inactive Chl to cope with future changes in PAR. The high nutrient use efficiency seems to be developed at the expense of low efficiency in water use (lower g_1). While we acknowledge this coordination warrants further examination of more species, it seems to be supported by some studies reporting that g_1 correlates positively to V_{cmax} (higher photosynthetic ability, lower water use efficiency) (Davidson et al., 2023). Therefore, our study provides a new venue for future studies to explore the potential of leveraging remote sensing-derived fluorescence (e.g., SIF) in modelling ecosystem water use.

4.5 | Potential of Chl *a*/*b* and Chl/Car in inferring photosynthetic capacity

Other than Φ(II), we have also explored other biochemical indicators (i.e., Chl *a* and *b*; Car) that might have reflected the allocation of photons for photosynthesis, and examined whether they can help improve the Chl-V_{cmax} relationship.

Chl *a*/*b* reflects the ratio of PS reaction centres to light-harvesting antennas (Kühlbrandt et al., 1994), and the ratio can potentially reflect the balance between light harvesting and conversion of the photosynthetic apparatus. We thus tested whether Chl *a*/*b* could serve as an alternative to Φ(II) in correcting for seasonal variation in the Chl-V_{cmax} relationship. However, several studies (Esteban et al., 2015; Poorter et al., 2019; Yu et al., 2022) found low plasticity of Chl *a*/*b* (<10%) after large changes in PAR at the weekly time-scale, at a much smaller extent than the changes in Φ(II). This observation is reinforced by our finding that Chl *a*/*b* is not significantly correlated to V_{cmax} or J_{max} (Supporting Information S1: Table 1), suggesting Chl *a*/*b* is unlikely to improve the Chl-V_{cmax} relationship.

Car not only participate in light harvesting (*β*-carotene) but also play a crucial role in photoprotection through the xanthophyll cycle (lutein and xanthophylls) (Esteban et al., 2015; Taiz et al., 2018). Chl/Car reflects light acclimation strategy through the balance between light harvesting and photoprotection (Förster et al., 2011; Havaux & Niyogi, 1999). We found that Chl/Car is significantly correlated to V_{cmax} and J_{max} (Supporting Information S1: Table 1), however, the r^2 is lower than that of Chl, indicating Car could not be used to improve the Chl-V_{cmax} relationship.

4.6 | Unexplained variations in V_{cmax}-Chl relationship and alternative approach to inferring V_{cmax} and Chl for remote sensing

Although our approach improved the accuracy of V_{cmax} and J_{max} estimation using Chl as a proxy, the reported r^2 values (0.55–0.74) suggest there remain variations in V_{cmax} and J_{max} that cannot be explained by Chl. These variations could be attributed to leaf age and ontogenetic stages (Brooks et al., 1996; Kimura et al., 1998; Rodriguez-Calcerrada et al., 2008). They could also be species-dependent, as species vary in their acclimation rates (Niinemets et al., 1998; Niinemets, 2020). Furthermore, the r^2 values from the V_{cmax}-Chl relationship of evergreen broadleaf forest leaves tend to be much lower (<0.4) than other PFTs, especially temperate deciduous and needleleaf forest leaves (mostly > 0.7) (Lu et al., 2022; Qian et al., 2021; Wang et al., 2020). This is likely associated with the small seasonal variations in light and thermal conditions in tropical areas, suggesting the need for taking leaf age or

ontogeny information into account to further constrain the V_{cmax}-Chl relationship.

Alternatively, spectroscopy approaches have been established to infer leaf biological and physiological properties such as leaf pigments, nitrogen, and photosynthetic capacity. (Dillen et al., 2012; Meacham-Hensold et al., 2020) demonstrated that partial least squares regression (PLSR) models based on hyperspectroscopy in visible, near-infra-red (NIR), and shortwave infra-red (SWIR) ranges could estimate V_{cmax} ($r^2 = 0.79$), J_{max}, ($r^2 = 0.59$) and Chl ($r^2 = 0.87$). Interestingly, the important spectral domains for V_{cmax} determination largely overlap with those for Chl (Serbin et al., 2012; Yan et al., 2021), reinforcing the basis of the empirical V_{cmax}-Chl relationship. However, caution should also be raised that these models require species- or site-dependent configuration, as was indicated by (Yan et al., 2021). In this study, r^2 values from V_{cmax} estimation range from 0.20 to 0.77 (median = 0.58) when site-specific models were applied to other sites. Moreover, spectroscopy studies often found higher accuracy of Chl determination than that of V_{cmax} and J_{max} (Asner & Martin, 2008; Meacham-Hensold et al., 2020), which could be due to low accuracy in inferring leaf nitrogen and a loose relationship between nitrogen and V_{cmax}. These uncertainties might need to be considered when using hyperspectroscopy to study the Chl-V_{cmax} and Chl-J_{max} relationships.

4.7 | Climate change impacts the Chl-V_{cmax} relationship

The Chl-V_{cmax} and Chl-J_{max} relationships might change under climate change since elevated CO_2 and temperature have been reported to impact J_{max} and V_{cmax} independently. A model-data comparison suggests a lowered V_{cmax} and an unchanged J_{max} under elevated CO_2 (Smith & Keenan, 2020). Meanwhile, higher temperatures would cause a decrease in J_{max} and an increase in V_{cmax} (Crous et al., 2022; Smith & Keenan, 2020). If we assume Chl is only sensitive to PAR (not to T and CO_2 changes, (Cave et al., 1981; Donnelly et al., 2001; León-Chan et al., 2017)), and PAR has not changed dramatically under climate change, we would expect a decrease in the Chl-V_{cmax} slope under elevated CO_2, and an increase in Chl-V_{cmax} slope and a decrease in Chl-J_{max} relationships under warming. Considering the current evidence, it would be necessary to include the impacts of climate change on the Chl-V_{cmax} relationship when utilising Chl in terrestrial biosphere models for photosynthesis simulations.

5 | CONCLUSION

In summary, using 5 years of observations of four deciduous tree species, we found strong seasonality in the relationship between leaf Chl and V_{cmax}. This seasonality is caused by the mismatch in the temporal scales at which V_{cmax} and Chl acclimate to light. We also found that the relationship between Chl and V_{cmax} could be strengthened by incorporating Chl fluorescence, as it reflects the effectiveness of light energy that is, harvested by Chl and used for driving the Calvin-Benson Cycle. Our study advances our understanding on the basis of the Chl-V_{cmax} relationship and the role of Chl in photosynthesis and sheds light on the application of Chl for large-scale carbon flux estimation.

ACKNOWLEDGEMENTS

Liyao Yu and Xiangzhong Luo are supported by the NUS Presidential Young Professorship awarded to Xiangzhong Luo (A-0003625-01-00). Holly Croft is supported by the UK Research and Innovation (UKRI) Future Leader Fellowship scheme (MR/T01993X/1).

CONFLICT OF INTEREST STATEMENT

The authors declare no conflict of interest.

DATA AVAILABILITY STATEMENT

Leaf photosynthetic and biochemical data will be available upon request to HC. Meteorological data can be accessed from Ameriflux (https://ameriflux.lbl.gov/). The code of the optimality photosynthesis model (in R) is available at https://github.com/SmithEcophysLab/optimal_vcmax_R.

ORCID

Liyao Yu http://orcid.org/0000-0002-6109-7462
Xiangzhong Luo http://orcid.org/0000-0002-9546-0960
Holly Croft http://orcid.org/0000-0002-1653-1071
Cheryl A. Rogers http://orcid.org/0000-0003-2792-1128
Jing M. Chen http://orcid.org/0000-0002-2143-6984

REFERENCES

Alton, P.B. (2017) Retrieval of seasonal Rubisco-limited photosynthetic capacity at global FLUXNET sites from hyperspectral satellite remote sensing: impact on carbon modelling. *Agricultural and Forest Meteorology*, 232, 74–88.

Anav, A., Friedlingstein, P., Beer, C., Ciais, P., Harper, A., Jones, C. et al. (2015) Spatiotemporal patterns of terrestrial gross primary production: a review. *Reviews of Geophysics*, 53, 785–818.

Asner, G. & Martin, R. (2008) Spectral and chemical analysis of tropical forests: scaling from leaf to canopy levels. *Remote Sensing of Environment*, 112, 3958–3970.

Bachofen, C., D'Odorico, P. & Buchmann, N. (2020) Light and VPD gradients drive foliar nitrogen partitioning and photosynthesis in the canopy of European beech and silver fir. *Oecologia*, 192, 323–339.

Björkman, O. & Holmgren, P. (1963) Adaptability of the photosynthetic apparatus to light intensity in ecotypes from exposed and shaded habitats. *Physiologia Plantarum*, 16, 889–914.

Boardman, N.K. (1977) Comparative photosynthesis of sun and shade plants. *Annual Review of Plant Physiology*, 28, 355–377.

Brooks, J., Sprugel, D.G. & Hinckley, T.M. (1996) The effects of light acclimation during and after foliage expansion on photosynthesis of *Abies amabilis* foliage within the canopy. *Oecologia*, 107, 21–32.

von Caemmerer, S. (2000) *Biochemical models of leaf photosynthesis*. Collingwood, Australia: CSIRO.

Cave, G., Tolley, L.C. & Strain, B.R. (1981) Effect of carbon dioxide enrichment on chlorophyll content, starch content and starch grain structure in *Trifolium subterraneum* leaves. *Physiologia Plantarum*, 51, 171–174.

Chen, J.-L., Reynolds, J.F., Harley, P.C. & Tenhunen, J.D. (1993) Coordination theory of leaf nitrogen distribution in a canopy. *Oecologia*, 93, 63–69.

Chen, J.M., Wang, R., Liu, Y., He, L., Croft, H., Luo, X. et al. (2022) Global datasets of leaf photosynthetic capacity for ecological and earth system research. *Earth System Science Data*, 14, 4077–4093.

Chen, Y.-E., Yuan, S., Lezhneva, L., Meurer, J., Schwenkert, S., Mamedov, F. et al. (2019) The low molecular mass photosystem II protein PsbTn is important for light acclimation. *Plant Physiology*, 179, 1739–1753.

Cowan, I.R. & Farquhar, G.D. (1977) Stomatal function in relation to leaf metabolism and environment. *Symposia of the Society for Experimental Biology*, 31, 471–505.

Croft, H., Chen, J.M., Luo, X., Bartlett, P., Chen, B. & Staebler, R.M. (2017) Leaf chlorophyll content as a proxy for leaf photosynthetic capacity. *Global Change Biology*, 23, 3513–3524.

Croft, H., Chen, J.M., Wang, R., Mo, G., Luo, S., Luo, X. et al. (2020) The global distribution of leaf chlorophyll content. *Remote Sensing of Environment*, 236, 111479.

Crous, K.Y., Uddling, J. & De Kauwe, M.G. (2022) Temperature responses of photosynthesis and respiration in evergreen trees from boreal to tropical latitudes. *New Phytologist*, 234, 353–374.

Davidson, K.J., Lamour, J., Rogers, A., Ely, K.S., Li, Q., McDowell, N.G. et al. (2023) Short-term variation in leaf-level water use efficiency in a tropical forest. *New Phytologist*, 237, 2069–2087.

Dillen, S.Y., de Beeck, M.O., Hufkens, K., Buonanduci, M. & Phillips, N.G. (2012) Seasonal patterns of foliar reflectance in relation to photosynthetic capacity and color index in two co-occurring tree species, *Quercus rubra* and *Betula papyrifera*. *Agricultural and Forest Meteorology*, 160, 60–68.

Donnelly, A., Craigon, J., Black, C.R., Colls, J.J. & Landon, G. (2001) Does elevated CO_2 ameliorate the impact of O_3 on chlorophyll content and photosynthesis in potato (*Solanum tuberosum*)? *Physiologia Plantarum*, 111, 501–511.

Dusenge, M.E., Madhavji, S. & Way, D.A. (2020) Contrasting acclimation responses to elevated CO_2 and warming between an evergreen and a deciduous boreal conifer. *Global Change Biology*, 26, 3639–3657.

Esteban, R., Barrutia, O., Artetxe, U., Fernández-Marín, B., Hernández, A. & García-Plazaola, J.I. (2015) Internal and external factors affecting photosynthetic pigment composition in plants: a meta-analytical approach. *New Phytologist*, 206, 268–280.

Evans, G.C. (1972) *The quantitative analysis of plant growth*. University of California Press

Evans, J.R. & Poorter, H. (2001) Photosynthetic acclimation of plants to growth irradiance: the relative importance of specific leaf area and nitrogen partitioning in maximizing carbon gain. *Plant, Cell & Environment*, 24, 755–767.

Farquhar, G.D., von Caemmerer, S. & Berry, J.A. (1980) A biochemical model of photosynthetic CO_2 assimilation in leaves of C_3 species. *Planta*, 149, 78–90.

Förster, B., Pogson, B.J. & Osmond, C.B. (2011) Lutein from deepoxidation of lutein epoxide replaces zeaxanthin to sustain an enhanced capacity for nonphotochemical chlorophyll fluorescence quenching in avocado shade leaves in the dark. *Plant Physiology*, 156, 393–403.

Friedlingstein, P., O'Sullivan, M., Jones, M.W., Andrew, R.M., Gregor, L., Hauck, J. et al. (2022) Global carbon budget 2022. *Earth System Science Data*, 14, 4811–4900.

Froelich, N., Croft, H., Chen, J.M., Gonsamo, A. & Staebler, R.M. (2015) Trends of carbon fluxes and climate over a mixed temperate–boreal transition forest in Southern Ontario, Canada. *Agricultural and Forest Meteorology*, 211-212, 72–84.

Genty, B., Briantais, J.M. & Baker, N.R. (1989) The relationship between the quantum yield of photosynthetic electron transport and quenching of chlorophyll fluorescence. *Biochimica et Biophysica Acta (BBA) - General Subjects*, 990, 87–92.

Goto, K., Yabuta, S., Ssenyonga, P., Tamaru, S. & Sakagami, J.-I. (2021) Response of leaf water potential, stomatal conductance and chlorophyll content under different levels of soil water, air vapor pressure deficit and solar radiation in chili pepper (*Capsicum chinense*). *Scientia Horticulturae*, 281, 109943.

Gu, J., Zhou, Z., Li, Z., Chen, Y., Wang, Z. & Zhang, H. (2017) Rice (*Oryza sativa* L.) with reduced chlorophyll content exhibit higher photosynthetic rate and efficiency, improved canopy light distribution, and greater yields than normally pigmented plants. *Field Crops Research*, 200, 58–70.

Havaux, M. & Niyogi, K.K. (1999) The violaxanthin cycle protects plants from photooxidative damage by more than one mechanism. *Proceedings of the National Academy of Sciences of the United States of America*, 96, 8762–8767.

He, L., Chen, J.M., Liu, J., Zheng, T., Wang, R., Joiner, J. et al. (2019) Diverse photosynthetic capacity of global ecosystems mapped by satellite chlorophyll fluorescence measurements. *Remote Sensing of Environment*, 232, 111344.

Houborg, R., F. McCabe, M., Cescatti, A. & A. Gitelson, A. (2015) Leaf chlorophyll constraint on model simulated gross primary productivity in agricultural systems. *International Journal of Applied Earth Observation and Geoinformation*, 43, 160–176.

Jiang, C., Ryu, Y., Wang, H. & Keenan, T.F. (2020) An optimality-based model explains seasonal variation in C_3 plant photosynthetic capacity. *Global Change Biology*, 26, 6493–6510.

Kattge, J. & Knorr, W. (2007) Temperature acclimation in a biochemical model of photosynthesis: a reanalysis of data from 36 species. *Plant, Cell & Environment*, 30, 1176–1190.

Kattge, J., Knorr, W., Raddatz, T. & Wirth, C. (2009) Quantifying photosynthetic capacity and its relationship to leaf nitrogen content for global-scale terrestrial biosphere models. *Global Change Biology*, 15, 976–991.

Kimura, K., Ishida, A., Uemura, A., Matsumoto, Y. & Terashima, I. (1998) Effects of current-year and previous-year PPFDs on shoot gross morphology and leaf properties in *Fagus japonica*. *Tree Physiology*, 18, 459–466.

Kong, L., Wen, Y., Jiao, X., Liu, X. & Xu, Z. (2021) Interactive regulation of light quality and temperature on cherry tomato growth and photosynthesis. *Environmental and Experimental Botany*, 182, 104326.

Kühlbrandt, W., Wang, D.N. & Fujiyoshi, Y. (1994) Atomic model of plant light-harvesting complex by electron crystallography. *Nature*, 367, 614–621.

León-Chan, R.G., López-Meyer, M., Osuna-Enciso, T., Sañudo-Barajas, J.A., Heredia, J.B. & León-Félix, J. (2017) Low temperature and ultraviolet-B radiation affect chlorophyll content and induce the accumulation of UV-B-absorbing and antioxidant compounds in bell pepper (*Capsicum annuum*) plants. *Environmental and Experimental Botany*, 139, 143–151.

Li, J., Lu, X., Ju, W., Li, J., Zhu, S. & Zhou, Y. (2022) Seasonal changes of leaf chlorophyll content as a proxy of photosynthetic capacity in winter wheat and paddy rice. *Ecological Indicators*, 140, 109018.

Li, J., Zhang, Y., Gu, L., Li, Z., Li, J., Zhang, Q. et al. (2020) Seasonal variations in the relationship between sun-induced chlorophyll fluorescence and photosynthetic capacity from the leaf to canopy level in a rice crop. *Journal of Experimental Botany*, 71, 7179–7197.

Li, Y., Ren, B., Gao, L., Ding, L., Jiang, D., Xu, X. et al. (2013) Less chlorophyll does not necessarily restrain light capture ability and photosynthesis in a chlorophyll-deficient rice mutant. *Journal of Agronomy and Crop Science*, 199, 49–56.

Lin, Y.-S., Medlyn, B.E., Duursma, R.A., Prentice, I.C., Wang, H., Baig, S. et al. (2015) Optimal stomatal behaviour around the world. *Nature Climate Change*, 5, 459–464.

Liu, Y., Chen, J.M., He, L., Wang, R., Smith, N.G., Keenan, T.F. et al. (2023) Global photosynthetic capacity of C_3 biomes retrieved from

solar-induced chlorophyll fluorescence and leaf chlorophyll content. *Remote Sensing of Environment*, 287, 113457.

Lu, X., Croft, H., Chen, J.M., Luo, Y. & Ju, W. (2022) Estimating photosynthetic capacity from optimized Rubisco–chlorophyll relationships among vegetation types and under global change. *Environmental Research Letters*, 17, 014028.

Luo, X., Croft, H., Chen, J.M., Bartlett, P., Staebler, R. & Froelich, N. (2018) Incorporating leaf chlorophyll content into a two-leaf terrestrial biosphere model for estimating carbon and water fluxes at a forest site. *Agricultural and Forest Meteorology*, 248, 156–168.

Luo, X., Croft, H., Chen, J.M., He, L. & Keenan, T.F. (2019) Improved estimates of global terrestrial photosynthesis using information on leaf chlorophyll content. *Global Change Biology*, 25, 2499–2514.

Luo, X. & Keenan, T.F. (2020) Global evidence for the acclimation of ecosystem photosynthesis to light. *Nature Ecology & Evolution*, 4, 1351–1357.

Maxwell, K. & Johnson, G.N. (2000) Chlorophyll fluorescence—a practical guide. *Journal of Experimental Botany*, 51, 659–668.

McConnaughay, K.D.M. & Coleman, J.S. (1999) Biomass allocation in plants: ontogeny or optimality? A test along three resource gradients. *Ecology*, 80, 2581–2593.

Meacham-Hensold, K., Fu, P., Wu, J., Serbin, S., Montes, C.M., Ainsworth, E. et al. (2020) Plot-level rapid screening for photosynthetic parameters using proximal hyperspectral imaging. *Journal of Experimental Botany*, 71, 2312–2328.

Medlyn, B.E., Duursma, R.A., Eamus, D., Ellsworth, D.S., Prentice, I.C., Barton, C.V.M. et al. (2011) Reconciling the optimal and empirical approaches to modelling stomatal conductance. *Global Change Biology*, 17, 2134–2144.

Miner, G.L. & Bauerle, W.L. (2019) Seasonal responses of photosynthetic parameters in maize and sunflower and their relationship with leaf functional traits. *Plant, Cell & Environment*, 42, 1561–1574.

Niinemets, Ü. (2020) Leaf trait plasticity and evolution in different plant functional types. *Annual Plant Reviews online*, 3, 473–522.

Niinemets, U., Kull, O. & Tenhunen, J.D. (1998) An analysis of light effects on foliar morphology, physiology, and light interception in temperate deciduous woody species of contrasting shade tolerance. *Tree Physiology*, 18, 681–696.

Niklas, K.J. (2006) A phyletic perspective on the allometry of plant biomass-partitioning patterns and functionally equivalent organ-categories. *New Phytologist*, 171, 27–40.

Oguchi, R., Hikosaka, K. & Hirose, T. (2005) Leaf anatomy as a constraint for photosynthetic acclimation: differential responses in leaf anatomy to increasing growth irradiance among three deciduous trees. *Plant, Cell & Environment*, 28, 916–927.

Pearcy, R.W., Krall, J.P. & Sassenrath-Cole, G.F. (1996) Photosynthesis in fluctuating light environments, *Photosynthesis and the environment*. Dordrecht: Kluwer Academic Publishers. pp. 321–346.

Piao, S., Sitch, S., Ciais, P., Friedlingstein, P., Peylin, P., Wang, X. et al. (2013) Evaluation of terrestrial carbon cycle models for their response to climate variability and to CO_2 trends. *Global Change Biology*, 19, 2117–2132.

Poorter, H., Niinemets, Ü., Ntagkas, N., Siebenkäs, A., Mäenpää, M., Matsubara, S. et al. (2019) A meta-analysis of plant responses to light intensity for 70 traits ranging from molecules to whole plant performance. *New Phytologist*, 223, 1073–1105.

Prentice, I.C., Dong, N., Gleason, S.M., Maire, V. & Wright, I.J. (2014) Balancing the costs of carbon gain and water transport: testing a new theoretical framework for plant functional ecology. *Ecology Letters*, 17, 82–91.

Qian, X., Liu, L., Croft, H. & Chen, J. (2021) Relationship between leaf maximum carboxylation rate and chlorophyll content preserved across 13 species. *Journal of Geophysical Research: Biogeosciences*, 126, e2020JG006076.

Rodriguez-Calcerrada, J., Reich, P.B., Rosenqvist, E., Pardos, J.A., Cano, F.J. & Aranda, I. (2008) Leaf physiological versus morphological acclimation to high-light exposure at different stages of foliar development in oak. *Tree Physiology*, 28, 761–771.

Rogers, A. (2014) The use and misuse of V(c,max) in earth system models. *Photosynthesis Research*, 119, 15–29.

Rogers, A., Medlyn, B.E., Dukes, J.S., Bonan, G., von Caemmerer, S., Dietze, M.C. et al. (2017) A roadmap for improving the representation of photosynthesis in earth system models. *New Phytologist*, 213, 22–42.

Ryu, Y., Berry, J.A. & Baldocchi, D.D. (2019) What is global photosynthesis? History, uncertainties and opportunities. *Remote Sensing of Environment*, 223, 95–114.

Schreiber, U., Schliwa, U. & Bilger, W. (1986) Continuous recording of photochemical and non-photochemical chlorophyll fluorescence quenching with a new type of modulation fluorometer. *Photosynthesis Research*, 10, 51–62.

Seemann, J.R., Sharkey, T.D., Wang, J. & Osmond, C.B. (1987) Environmental effects on photosynthesis, nitrogen-use efficiency, and metabolite pools in leaves of sun and shade plants. *Plant Physiology*, 84, 796–802.

Serbin, S.P., Dillaway, D.N., Kruger, E.L. & Townsend, P.A. (2012) Leaf optical properties reflect variation in photosynthetic metabolism and its sensitivity to temperature. *Journal of Experimental Botany*, 63, 489–502.

Smith, N.G. & Keenan, T.F. (2020) Mechanisms underlying leaf photosynthetic acclimation to warming and elevated CO_2 as inferred from least-cost optimality theory. *Global Change Biology*, 26, 5202–5216.

Smith, N.G., Keenan, T.F., Colin Prentice, I., Wang, H., Wright, I.J., Niinemets, Ü. et al. (2019) Global photosynthetic capacity is optimized to the environment. *Ecology Letters*, 22, 506–517.

Sonoike, K., (2011) Photoinhibition of photosystem I. *Physiologia Plantarum*, 142, 56–64.

Sun, H., Zhang, S.B., Liu, T. & Huang, W. (2020) Decreased photosystem II activity facilitates acclimation to fluctuating light in the understory plant *Paris polyphylla*. *Biochimica et Biophysica Acta (BBA) - Bioenergetics*, 1861, 148135.

Taiz, L., Zeiger, E., Møller, I.M. & Murphy, A.S. (2018) *Fundamentals of plant physiology*. Oxford University Press

Terashima, I., Miyazawa, S.-I. & Hanba, Y.T. (2001) Why are sun leaves thicker than shade leaves?—consideration based on analyses of CO_2 diffusion in the leaf. *Journal of Plant Research*, 114, 93–105.

De la Torre, W.R. & Burkey, K.O. (1990) Acclimation of barley to changes in light intensity: chlorophyll organization. *Photosynthesis Research*, 24, 117–125.

Uemura, A., Ishida, A., Nakano, T., Terashima, I., Tanabe, H. & Matsumoto, Y. (2000) Acclimation of leaf characteristics of *Fagus* species to previous-year and current-year solar irradiances. *Tree Physiology*, 20, 945–951.

Walker, A.P., Quaife, T., van Bodegom, P.M., De Kauwe, M.G., Keenan, T.F. & Joiner, J. et al. (2017) The impact of alternative trait-scaling hypotheses for the maximum photosynthetic carboxylation rate (V_{cmax}) on global gross primary production. *New Phytologist*, 215, 1370–1386.

Walters, R. & Horton, P. (1995) Acclimation of *Arabidopsis thaliana* to the light environment: changes in photosynthetic function. *Planta*, 197, 306–312.

Wang, G., Zeng, F., Song, P., Sun, B., Wang, Q. & Wang, J. (2022) Effects of reduced chlorophyll content on photosystem functions and photosynthetic electron transport rate in rice leaves. *Journal of Plant Physiology*, 272, 153669.

Wang, S., Li, Y., Ju, W., Chen, B., Chen, J., Croft, H. et al. (2020) Estimation of leaf photosynthetic capacity from leaf chlorophyll content and leaf age in a subtropical evergreen coniferous

plantation. *Journal of Geophysical Research: Biogeosciences*, 125, e2019JG005020.

Warren, C.R. (2006) Why does photosynthesis decrease with needle age in *Pinus pinaster*? *Trees*, 20, 157–164.

Wieneke, S., Balzarolo, M., Asard, H., Abd Elgawad, H., Peñuelas, J., Rascher, U. et al. (2022) Fluorescence ratio and photochemical reflectance index as a proxy for photosynthetic quantum efficiency of photosystem II along a phosphorus gradient. *Agricultural and Forest Meteorology*, 322, 109019.

Wong, S.C., Cowan, I.R. & Farquhar, G.D. (1979) Stomatal conductance correlates with photosynthetic capacity. *Nature*, 282, 424–426.

Wullschleger, S.D. (1993) Biochemical limitations to carbon assimilation in C_3 plants—a retrospective analysis of the A/C_i curves from 109 species. *Journal of Experimental Botany*, 44, 907–920.

Wyka, T.P., Robakowski, P., Żytkowiak, R. & Oleksyn, J. (2022) Anatomical acclimation of mature leaves to increased irradiance in sycamore maple (*Acer pseudoplatanus* L.). *Photosynthesis Research*, 154, 41–55.

Xie, J., Tang, L., Wang, Z., Xu, G. & Li, Y. (2012) Distinguishing the biomass allocation variance resulting from ontogenetic drift or acclimation to soil texture. *PLoS One*, 7, e41502.

Xu, M., Liu, R., Chen, J.M., Liu, Y., Wolanin, A., Croft, H. et al. (2022) A 21-year time series of global leaf chlorophyll content maps from MODIS imagery. *IEEE Transactions on Geoscience and Remote Sensing*, 60, 1–13.

Yamashita, N., Koike, N. & Ishida, A. (2002) Leaf ontogenetic dependence of light acclimation in invasive and native subtropical trees of different successional status. *Plant, Cell & Environment*, 25, 1341–1356.

Yan, Z., Guo, Z., Serbin, S.P., Song, G., Zhao, Y., Chen, Y. et al. (2021) Spectroscopy outperforms leaf trait relationships for predicting photosynthetic capacity across different forest types. *New Phytologist*, 232, 134–147.

Yu, L., Fujiwara, K. & Matsuda, R. (2022) Estimating light acclimation parameters of cucumber leaves using time-weighted averages of daily photosynthetic photon flux density. *Frontiers in Plant Science*, 12, 809046.

Zhang, Y., Guanter, L., Berry, J.A., Joiner, J., van der Tol, C., Huete, A. et al. (2014) Estimation of vegetation photosynthetic capacity from space-based measurements of chlorophyll fluorescence for terrestrial biosphere models. *Global Change Biology*, 20, 3727–3742.

Zhou, Z., Struik, P.C., Gu, J., van der Putten, P.E.L., Wang, Z. & Yin, X. et al. (2023) Enhancing leaf photosynthesis from altered chlorophyll content requires optimal partitioning of nitrogen. *Crop and Environment*, 2, 24–36.

SUPPORTING INFORMATION

Additional supporting information can be found online in the Supporting Information section at the end of this article.

How to cite this article: Yu, L., Luo, X., Croft, H., Rogers, C. A. & Chen, J. M. (2024) Seasonal variation in the relationship between leaf chlorophyll content and photosynthetic capacity. *Plant, Cell & Environment*, 1–13. https://doi.org/10.1111/pce.14997